JOURNAL OF MATERIALS SCIENCE 29 (1994) 1527–1532

Novel approaches in the melt-texturing of $YBa_2Cu_3O_{7-y}$

R. V. KUMAR, D. J. FRAY
Department of Mining and Mineral Engineering, University of Leeds, Leeds, UK
H. W. WILLIAMS, A. MISSON, J. E. EVETTS
Department of Materials Science and Metallurgy, University of Cambridge, Cambridge, UK

Electrochemically pre-textured samples have been subjected to melt-processing in order to produce dense and highly textured bulk samples of $YBa_2Cu_3O_{7-y}$ (YBCO). Full oxygenation of these samples has been achieved at high processing temperatures of 720 °C by electrochemical titration, in order to increase the superconducting transition temperature to > 89 K. These samples show a large magnetic hysteresis, and the value of J_c calculated using the Bean model is in the range 4000–6000 A cm^{-2} at 77 K and 1 tesla magnetic field, and is independent of the applied field in that range. In another variation of the melt-processing technique — referred to as "isothermal melt-textured growth" — highly textured samples have been produced by the movement of the solidification front at a constant temperature in an oxygen activity gradient.

1. Introduction

Prospects for application of high-T_c superconducting oxides are astounding in several fields, such as power transmission, energy storage, levitation, magnetic shielding, infra-red sensors and microelectronics. Practical application of bulk high-T_c ceramic superconductors are currently hampered by low values of critical current density (J_c), especially in strong magnetic fields. In contrast, it is possible to obtain very high J_c in single crystals and thin films [1, 2]. In order to achieve high J_c at liquid nitrogen temperatures, the bulk superconductor must simultaneously satisfy all the following criteria.

(i) Optimum oxygen content in YBCO in the entire bulk sample to achieve maximum T_c [3].
(ii) Absence of large grains of second phases detrimental to the superconducting properties.
(iii) High density of samples (> 95%).
(iv) Crystallographic alignment of large grains parallel to the a–b conduction planes.
(v) Elimination or minimization of weak-link high-angle grain boundaries in the path of current flow.
(vi) Good connectivity between grains across both high-angle and low-angle boundaries.
(vii) Incorporation of flux pinning centres in order to reduce field-dependent deterioration of J_c in high magnetic fields.

Oxygen and phase control in YBCO are normally achieved by high-temperature sintering (> 930 °C) and annealing (< 550 °C). In a previous publication [3], we have reported the use of high-temperature electrochemical processing for the precise and optimal control of oxygen content as well as phase control in YBCO. The electrochemical device consists of both coulometric and potentiometric modes and can be described by the cell represented in Fig. 1. The coulometric part of the electrochemical cell represents an oxygen pump for varying the oxygen input to or removal from YBCO, while the potentiometric part acts as an oxygen sensor for monitoring the oxygen potential in YBCO. This technique has been successfully applied to YBCO for oxygen control at high temperatures and in the development of phase stability diagrams [3].

Furthermore, we also reported significant texture enhancement in the electrochemically treated YBCO bulk samples, provided the morphology of the starting powder is favourable [3]. It was observed that enhanced c-axis texture can be obtained in the bulk-sintered samples of YBCO by the combined effect of pressure, temperature and electrochemical potential. The sample is squeezed by a pressure of

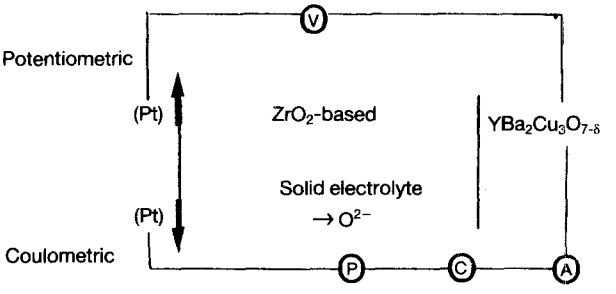

Figure 1 The electrochemical cell. V = high-impedance voltmeter which measures emf in an open circuit; P = potentiostat for application of suitable potential or current; C = coulometer for measuring the amount of oxygen transported through the solid electrolyte; A = ammeter for measuring the rate of oxygen transported through the device.

0022–2461

$> 1.2\,kg\,mm^{-2}$ in the temperature range 700–960 °C, and with oxygen pressures corresponding to the decomposition of YBCO as indicated by the 'emf plateaux'. In addition to these conditions, the role of morphology of precursor powders has proved crucial in determining the response of texture enhancement. The best results are obtained for powders with grains that are platelet-like with high aspect ratio, and for very finely sized reactive precursor with the high aspect ratio particles as seed material. The exact mechanism for the texture formation is not clear. The following possibilities either singly or in combination can be considered: (i) liquidus formation due to decomposition of YBCO which enhances grain growth anisotropy [4]; (ii) force-induced movement of YBCO grains in the presence of liquid phase [5]; (iii) decomposition of YBCO (1 2 3 phase) to the 1 2 4 phase and recrystallization of YBCO with preferred orientation [6]. Further research is required to elucidate the mechanism of texture formation by this technique.

In general, it was found that there is a strong correlation between texture enhancement by electrochemical processing and the ability of the material to exhibit large grain growth in normal sintering. Samples which exhibit good grain growth during sintering respond favourably to electrochemical texturing, and *vice versa*. Good grain growth was obtained in samples made of powders with grains that are platelet-like with high aspect ratios. On the other hand, the densities of samples with large grains were generally found to be unacceptably low.

In this study, YBCO powders from a variety of sources were used and were characterized for their size distribution (particle size analyser), morphology (scaning electronmicroscopy; SEM), chemical and phase composition (X-ray diffraction; XRD, energy-dispersive spectroscopy, EDX, and chemical analysis) and liquidus temperatures (differential thermal analysis; DTA) (see Table I). Bulk samples prepared by pressing and sintering were subject to electrochemical treatment in a cell holder shown in Fig. 2. Oxygen titration was carried out symmetrically from both the flat surfaces of YBCO pellet using two identical YSZ solid electrolytes [3]. The experimental details and the results are described in [3].

The texture factor of the YBCO samples was calculated from the XRD intensity ratios $I_{0\,0\,6}/I_{1\,1\,0,\,1\,0\,3}$, of the sample and a reference powder [7]. The best

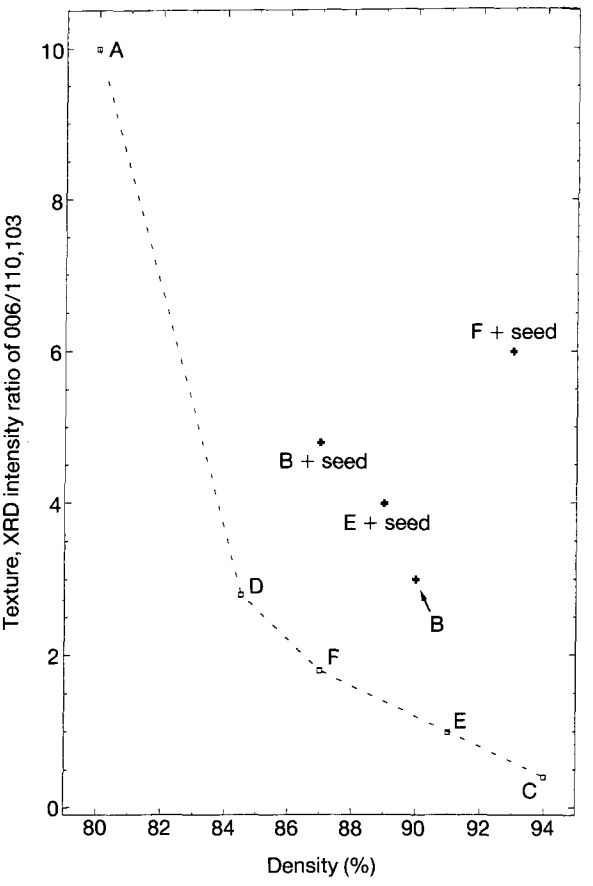

Figure 2 Texture in YBCO (EC).

results were obtained for YBCO powders with coarse grains and high aspect ratio platelets ($I_{0\,0\,6}/I_{1\,1\,0,\,1\,0\,3} = 10$ for sample A). Despite achieving good texturing, transport currents in these samples are very low ($10\,A\,cm^{-2}$ at 77 K and 1 tesla) due to their high porosity (20%), which severely restricts the current paths. However, by seeding fine precursor powders with coarse particles, it was possible to achieve fairly good texture in a high density material (sample F + seed).

These results are summarized in Fig. 3, which indicates the combination of texture and density achieved in the electrochemically (EC)-treated samples. Best results so far have been obtained by seeding the powder F with coarse powder A, where bulk samples with densities approaching 95% have been electrochemically treated to obtain reasonably good texture ($I_{0\,0\,6}/I_{1\,1\,0,\,1\,0\,3} = 6$).

TABLE I Properties of precursor powders

Powder*	Average particle size (μm)	Particle shape	Chemical composition	Liquidus temperature (°C)
A	20	Elongated platelets with high aspect ratios	Excess Ba and Cu	1038, 990
B	5	Ground	Excess Ba and Cu	1036, 987
C	2	Uniform spherical particles	High in S (0.25%)	1020, 960, 925
D	10	Angular particles	High in 2nd phases	1035, 970, 950, 925
E	5	Rod-shaped	Excess Ba and Cu	1033, 925
F	3	Mostly globular	High in C	1036, 981

* Sample A prepared in this laboratory; sample B prepared by grinding sample A; samples C to F obtained from commercial sources.

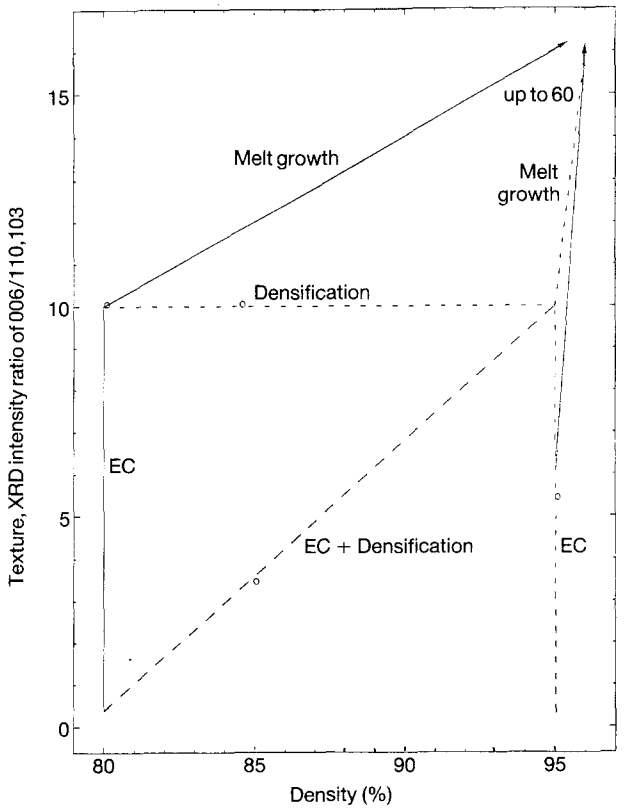

Figure 3 Texture and density in YBCO.

2. Partial melt processing

Samples that are fairly dense as well as reasonably textured (e.g. F + seed) show improved microstructure in terms of porosity, grain alignment and connectivity (Fig. 4). These improvements, however, have translated into only a marginal increase in transport current densities (360 A cm^{-2}), which indicate that despite substantial increase in density and texture, weak-link features have not been eliminated from the bulk samples. It has been suggested that the only proven technique for eliminating the severe weak-link behaviour in YBCO bulk samples is the use of melt processing techniques [8–10]. Therefore, we have incorporated a partial-melt processing method to treat an electrochemically pre-textured bulk sample in order to maximize texture in dense samples, to eliminate severe weak links and to promote the formation of flux-pinning centres. One of the advantages of using pre-textured samples is that a short partial melting stage is sufficient, in order mainly to melt the untextured fine grains, and promote their growth on the existing habit planes of the large-textured grains. This greatly minimizes some of the frequently encountered problems in melt texturing of YBCO, such as chemical reaction with the substrate and warping of the bulk sample.

The procedure basically involves a directional solidification process of the YBCO phase from a partial-melt state. An electrochemically pre-textured sample is heated in an oxygen atmosphere to a temperature slightly above the peritectic temperature for decomposition into a CuO-rich liquid and Y_2BaCuO_5 (Fig. 5), and slowly cooled at 1 °C h^{-1} from about 1035 to 925 °C for nucleation and growth of the YBCO phase, and then rapidly cooled to room temperature, without the usual oxygenation anneal at temperatures < 550 ° C.

Dense bulk samples (95%) with extremely high texture ($I_{0\,0\,6}/I_{1\,1\,0,\,1\,0\,3} = 60$), which easily maintain their structural integrity, have been produced by this process (Figs 3 and 6). T_c measurements, however, indicated that the samples were not fully oxygenated and the values varied in the 79–82 K range.

3. Electrochemical oxygenation

Full oxygenation of very dense samples requires very long anneals at temperatures < 550 °C. In order to maximize T_c, annealing in pure oxygen atmosphere must be carried out at temperatures near 400 °C, at which the kinetics are extremely unfavourable, as can be seen from the calculations based on diffusion data (Table II). Furthermore, during such an anneal, it is

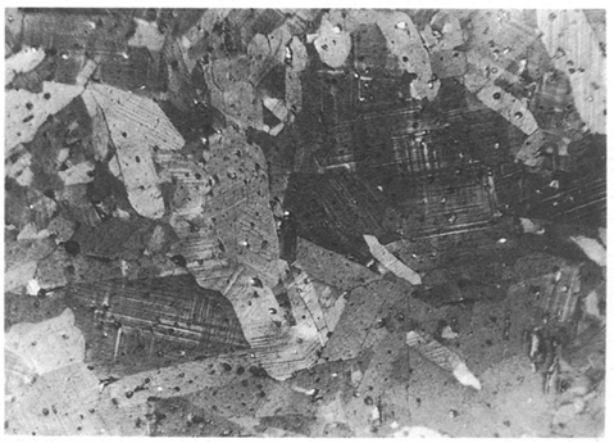

Figure 4 Optical microstructure of electrochemically textured sample (F + Seed) (× 500).

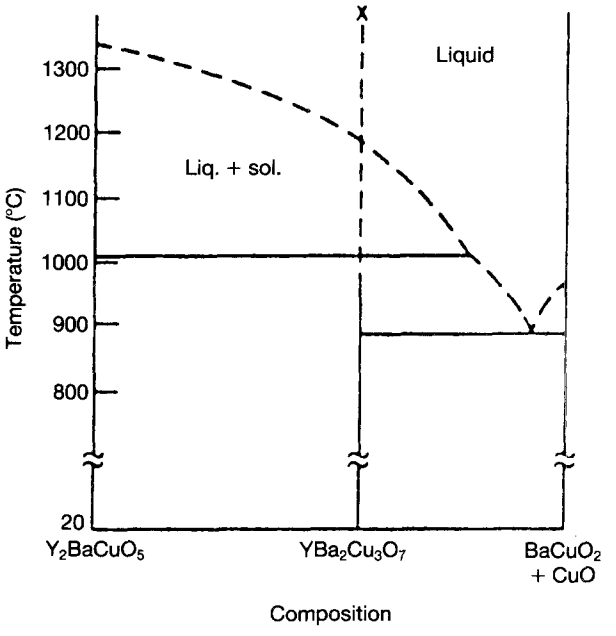

Figure 5 The Y_2BaCuO_5–$BaCuO_2$ + CuO phase diagram.

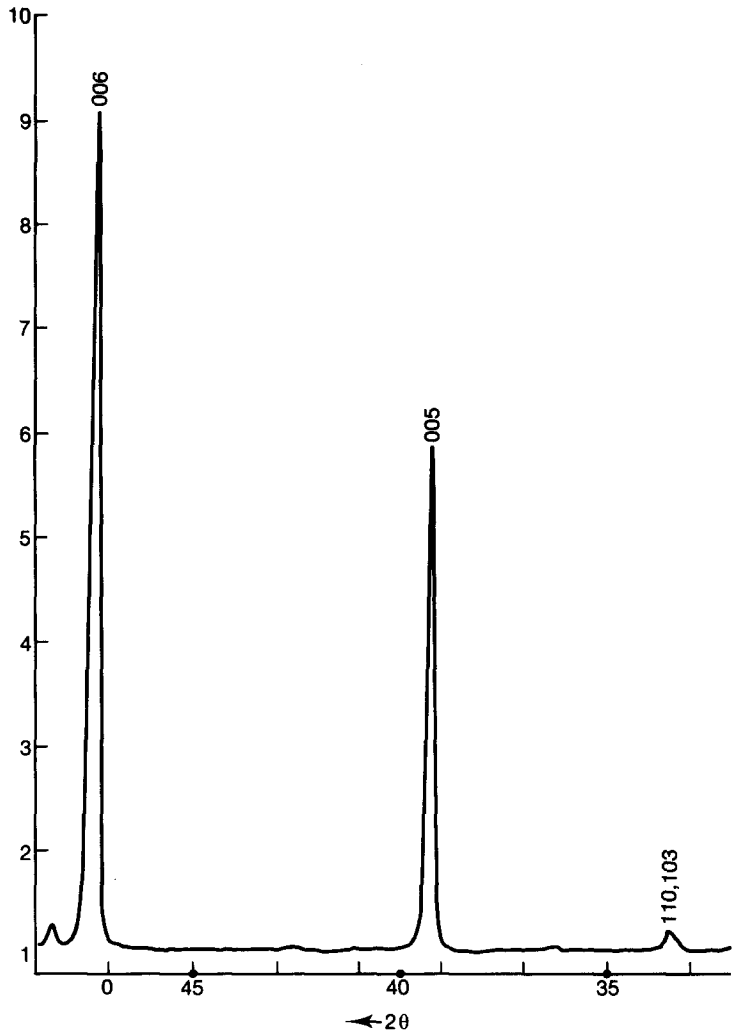

Figure 6 XRD Pattern for a highly textured sample by partial melt processing of EC textured samples.

not possible to monitor the extent of oxygenation, and usually very long anneals are used.

In a previous publication [3], we have reported the application of an electrochemical technique of oxygenating YBCO, accompanied by the simultaneous monitoring of the extent of this oxygenation. In addition, it is possible to create electrochemical variation of activities covering a wide range of compositions, not easily attained by the use of gas pressure. Dense and highly textured samples from this study were electrochemically oxygenated in less than 3 h at a relatively a high processing temperature of 720 °C, at which the benefits of rapid-reaction kinetics could be fully exploited. By this method the superconducting transition temperature of the melt-textured YBCO samples was increased from the 79–82 K to the 89–92 K range.

TABLE II Oxygen diffusion data (atmospheric O_2) for dense MTG samples (> 95%)

Temperature	Time to fully oxygenate to depth d:			
	10 nm	1 μm	0.1 mm	10 mm
400 °C	50 ms	500 s	60 days	2000 y
600 °C	0.005 ms	50 ms	500 s	60 days

T_c increased from 79–82 K to > 89 K after electrochemical oxygenation at 720 °C.

4. Magnetization measurement of critical current

YBCO samples were subject to magnetization measurements on an Aerosonic 3001 VSM (vibrating sample magnetometer) using an Oxford Instruments flow cryostat to determine the critical current densities. Magnetization measurements were conducted as the sample thickness was reduced. According to the Bean critical state model [11], the difference in magnetization (M^+-M^-) between the increasing and the decreasing applied field (H) branches is related to sample thickness d by the following relationship:

$$M = M^+-M^- = J_c\, d/20 \qquad (1)$$

where J_c is in A cm^{-2}, M in emu cm^{-3} and d in cm. Therefore, the value of the critical current is obtained from the slope of M–d lines.

The M–d lines for samples prior to melt treatment have very low J_c values as estimated from the slopes (Fig. 7), indicating the presence of weak links which greatly diminish the conduction paths. Using the theoretical limit of maximum magnetization current, the characteristic superconducting dimension can be estimated to be at least two orders of magnitude larger than the grain size. This is strong evidence that macroscopic currents encompassing a large number of grains can flow through the sample.

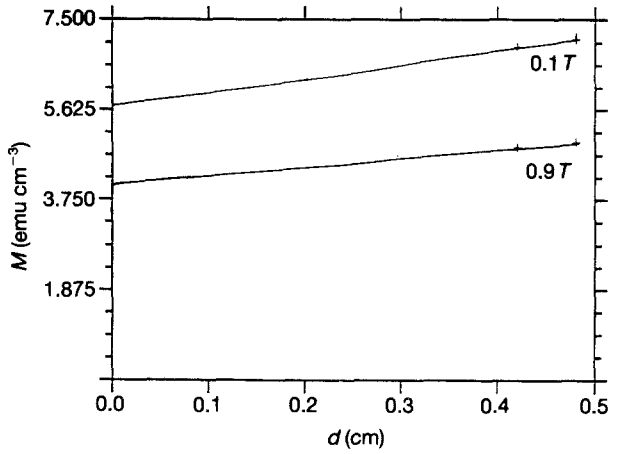

Figure 7 Magnetization against thickness for samples prior to partial melt texturing.

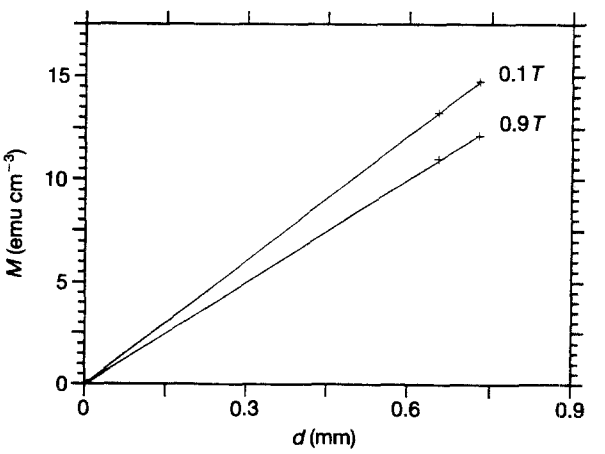

Figure 9 Magnetization against thickness for a melt-textured YBCO sample, showing fully inter-granular currents.

Rectangular samples of approximately 5 × 3.5 × 1 mm were cut from the melt-textured and electrochemically oxygenated sample for VSM measurements. These samples show a large magnetic hysteresis at 77 K and exhibit a persistent-current-based magnet-like behaviour even after the field is removed (Fig. 8). From the M–H loops for the electrochemically oxygenated melt-textured samples, derived as a function of sample thickness, it can be seen that the Bean critical state is established, which implies that the supercurrents circulate in the entire bulk sample, and that the weak links are absent (Fig. 9). The value of J_c as calculated from the Bean model varied from 4000–6000 A cm^{-2} at 77 K and 1 tesla field, and is independent of the applied field in that range.

5. Isothermal melt-textured growth

The variety of melt-texturing techniques reported in the literature for aligning YBCO grains in a bulk sample is essentially based on the slow cooling of the sample near the peritectic temperatures, either with or without a temperature gradient [8–12]. Growth of YBCO crystals in a liquid flux leads to the formation of thin platelets as a result of the faster rate of growth in the a–b direction than in the c-direction of the crystal. Slow cooling through the peritectic, especially in the presence of a temperature gradient, controls the morphology of the solidification interface to produce domains of highly textured grains. The different versions of these reported melt-texturing process are all carried out at a fixed oxygen pressure, usually at 1 atm.

In a suggested new process, variation of the liquidus temperature with oxygen activity is exploited for the growth of aligned crystallites under isothermal conditions. The oxygen pressure has a pronounced effect on the peritectic temperature. For a change of pressure from 1 to 0.02 atm, the peritectic temperature decreases by ~ 50 °C [3, 13]. Decrease in the oxygen activity is also accompanied by a decrease in the steepness of the liquidus line between the peritectic and the eutectic temperature in the Y_2BaCuO_5–$YBa_2Cu_3O_{7-y}$–$3BaCuO_2 + 2CuO$ join of the Y_2O_3–BaO–CuO phase diagram (Fig. 4) [14], which creates more favourable conditions for the growth of large crystals.

In preliminary experiments, highly textured grains in a bulk YBCO sample were produced by gradually increasing the oxygen pressure of the gaseous atmosphere from 0.02 to 1 atm, at a constant temperature of 1030 °C. Highly aligned tracks of crystallites were produced in the sample, along with a distribution of discrete particles of 2 1 1 as well as 15–20 vol % of the green phase (2 2 1). The microstructures obtained for the isothermally textured samples are similar to those obtained by the normal melt-textured techniques (Figs 10 and 11). Both samples show a near-perfect alignment of the superconducting phase. Polarized optical microscopic observations clearly indicate the presence of twins. The textured tracks are at an angle of 30–50° with respect to the sample axis, indicating complex heat and mass-transfer criteria governing the movement of the solidification front under the oxygen activity gradient. Further work is being carried out to investigate the application of electrochemical techniques to create the required oxygen activity gradient, in order to form a track of highly textured superconducting phase in a YBCO sample.

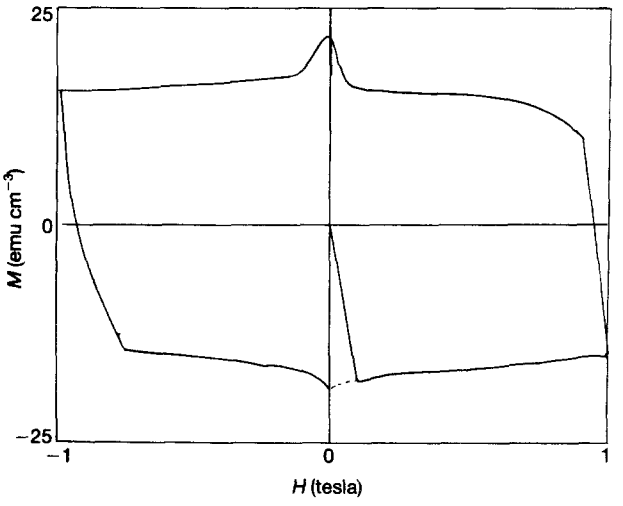

Figure 8 Magnetization curve for a melt-textured sample.

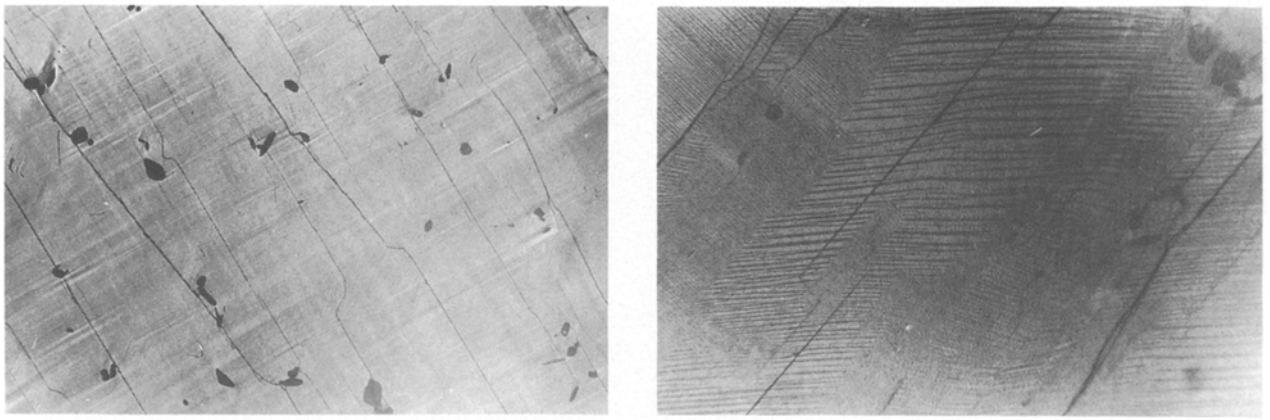

Figure 10 Optical microstructures of melt-textured YBCO samples (× 500).

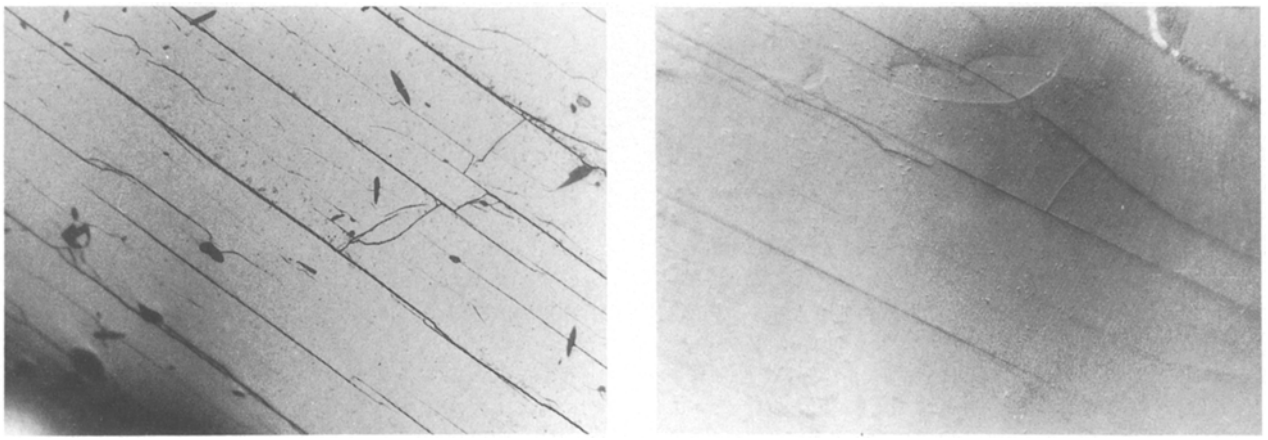

Figure 11 Optical microstructures of isothermally melt-textured YBCO samples (× 500).

6. Conclusions

A processing route, which optimizes the properties of bulk samples of YBCO by maximizing the benefits of coulometric oxygenation, electrochemical texturing and melt-processing, has been considered, with encouraging results.

FABRICATION
↓
SINTERING
↓
ELECTROCHEMICAL PRETEXTURING AND OXYGENATION
↓
(ELECTROCHEMICAL) MELT GROWTH FOR TEXTURING, DENSIFICATION AND GRAIN GROWTH
↓
ELECTROCHEMICAL OXYGENATION

The variation of liquidus temperature with oxygen activity is exploited in the development of isothermal melt-textured growth of YBCO, and can be interfaced with electrochemical cells for developing textured tracks in a bulk YBCO sample.

Acknowledgements

The authors would like to thank Cambridge Advanced Materials, Cookson Technology Centre, Oxford Instruments and the UK Department of Trade and Industry for their financial support and technical collaboration.

References

1. P. CHAUDHARY, R. M. KOCH, R. B. LAIBOWITZ, J. R. McGUIRE and R. J. GAMBINO, *Phys. Rev. Lett.* **58** (1987) 2684.
2. L. F. SCHEENMEYER, E. M. GYORGY and J. V. WASZEZAK, *Phys. Rev.* **34B** (1981) 8804.
3. R. V. KUMAR, D. J. FRAY, J. E. EVETTS, H. W. WILLIAMS and A. MISSON, *J. Electrochem Soc.* **43** (1993) 1285.
4. S. R. SU, M. O'CONNOR and M. LEVINSON, *J. Mater. Res.*, **6** (1991) 244.
5. P. REGINIER, L. CHAFFRON, X. DESCHARELS and L. SCHMIRGELD, in Proceedings of the 7th CIMTEC World Ceramic Congress, Satellite Symposium 4, HTC Superconductors, Trieste, 2–5 July 1990.
6. R. RAMESH, *Nature* **346** (1990) 420.
7. F. K. LOTGERING, *J. Inorg. Nucl. Chem.* **9** (1959) 113.
8. S. JIN and J. E. GRAEBNER, *Mater. Sci. and Engng.* **B7** (1991) 243.
9. S. JIN, *J. Metals* **43** (1991) 7.
10. P. J. McGINN, W. CHEN and N. ZHU, *J. Metals* **43** (1991) 26.
11. M. MURUKAMI, M. MORITA and N. KOYAMA, *Jpn J. Appl. Phys.* **26** (1989) L1125.
12. K. SALAMA, V. SELVAMANICKAM, L. GAO and K. SUN, *Appl. Phys. Lett.* **54** (1989) 2352.
13. B-J. LEE and D. N. LEE, *J. Amer. Ceran. Soc.* **74** (1991) 78.
14. *Idem, ibid.* **72** (1989) 314.

Received 23 September 1992
and accepted 27 September 1993